RSC Advances

ROYAL SOCIETY OF CHEMISTRY

www.rsc.org/advances

RSC Advances

ARTICLE

Synthesis of novel monolithic activated carbons from phenol–urea–formaldehyde resin

Received 00th January 20xx,
Accepted 00th January 20xx

DOI: 10.1039/x0xx00000x

www.rsc.org/

W. ZHAO,[a*] H. Gao[a] and M. Fan[b]

The phenol–urea–formaldehyde (PUF) organic foams have been firstly synthesized from phenol–urea–formaldehyde resin under alkali condition. Carbonization and CO_2 activation were then used to prepare a novel monolithic nitrogen-containing activated carbon foam with both interconnected macroporous and micro/meso- porosity structures from the developed PUF organic foam. The macroporosity produced from the organic foams, which corresponds to the connected network of cells, has diameter in the range of 100-600um. The micro/meso-porosity produced by activation is located at the inner surface of the cells. The developed carbons have achieved apparent surface area as high as 1674m^2/g and microporous volume as high as 0.86cm^3/g, which are similar to that of many commercial carbonaceous adsorbents, but with nitrogen content around 1.5 wt. %. These activated carbon foams were expected to have higher adsorption kinetics and some special applications due to the heteroatom nitrogen introduced and the bimodal cellular structure.

Introduction

Activated carbons (ACs) are materials of critical importance for industrial applications due to the abundant pore structure and high surface area. The features give them the potential for using as adsorbents, catalyst supports, energy storage and biological materials in various industry areas [1-4].

While any cheap material having high carbon element and moderate inorganic contents can be used for ACs production, activated carbons produced from coal, petroleum, vegetable and polymeric precursors have played a major role as raw materials [5]. The problems with conventional precursors will tend to limit the purity, strength and the physical form of the product materials. It seems likely that these will only be overcome by the use of polymeric precursors, where the reproducibility and purity of the precursor is within the control of the manufacturer and the physical forms and structure can be tailored through the polymer production process [48]. Thus, synthetic polymers-based activated carbons are extensively investigated nowadays [33-36,43-47]. Phenol-formaldehyde resin (PF) has lower ash content and provides a variety of product forms, such as fiber, foam, granular even monolithic structures, which are usually used as polymeric precursor to prepare activated carbons [6-9]. In wood industry, urea was incorporated with phenol and formaldehyde in an alkaline environment to prepare the widely known 'phenol-formaldehyde-urea (PUF) cocondensed resins' by polycondensation [10-13]. Due to the high content of nitrogen, PUF resin can replace the PF resin and be employed as precursor or nitrogen resource to fabricate the nitrogen containing PUF foams, and then PUF activated carbon foams. This is because the obtained PUF foams usually were in a low surface area with macropores and therefore needed the activation process to produce micro/meso- porosity. So the first advantage of using PUF foams as precursor is the heteroatom nitrogen introduced by urea addition in the raw material. This functional activated carbon foams with nitrogen doped can directly synthesize by copolymerizztion, without the post-modification. The existence of heteroelements in activated carbon foams may significantly alter the electronic structure, thus affecting the interaction between carbon and adsorbed gas or liquid, and enhancing the performance of the applications [14-16, 33].

ACs are normally in the form of grains or granular whose surface area is mainly controlled by their inner microporosity (pore size less than 2nm) and mesoporosity (pore size in the range of 2 to 50 nm) [17]. The mesoporosity also plays the role of the pathways for reactants flowing throughout carbon grains, but mesoporosity is highly tortuous and its corresponding volume may not be high enough. As mentioned, the PUF activated carbon foams can prepared from PUF foams, which usually has low density, high porosity and cell dimension more than 100 um, but with very low surface area [18-19]. So the other advantage of using PUF foams as precursor is that the prepared monolithic activated carbon foams were provided with bimodal cellular structure. It containing both interconnected macroporous from PUF foams and micro/meso- porosity structures from activation process, give them the distinct advantages such as low pressure drop, fast heat and mass transfer, high contacting efficiency and easy to deal with, so has attracted much attention for potential applications in many science and engineering sectors [8, 20-21, 33].

[a] College of Material Engineering, Fujian Agriculture and Forestry University, NO 15 Shangxiadian Road, Fuzhou 350002, PR China
[b] College of Engineering Design and Physical Sciences, Brunel University, Uxbridge UB8 3PH, United Kingdom

The present work was firstly to synthesize organic foams from phenol-urea-formaldehyde resin with phenol, urea and formaldehyde under alkali condition, and then to carbonize and activate them for preparing novel monolithic nitrogen-containing activated carbon foams with bimodal cellular structure. The microstructures, compression strength and sorption behaviour were then characterized for possible application as energy storage, catalyst support, adsorbent. The key features of this new material are: firstly, the functional activated carbon foams with nitrogen doped were synthesized directly by copolymerization. Once the precursor is provided, only one-step activation under inert gas atmosphere is necessary for heteroatom-doped carbons production, thus without the post-modification. The other is the monolithic activated carbon with bimodal cellular structure, gives them the distinct advantages such as low pressure drop, fast heat and mass transfer, high contacting efficiency and easy to deal with.

Experimental

Materials: The following materials were used in the PUF resin and foam production: phenol, formaldehyde, sodium carbonate anhydrous, urea, tween 80, n-Pentane and p-toluene sulfonic acid (pTSA) which were all purchased from Fuzhou Xinyuhua Chemistry and Laboratory Apparatus Co., Ltd. (China). All reagents were analytic grade and used without further purification or treatment.

Synthesis of PUF resin: Phenol, urea and 37% formaldehyde with a mole ratio of 1:0.25:1.8 were mixed and added to a 250mL, three-necked flask fitted with a condenser and a mechanical stirrer. The pH was adjusted to about 9-10 with an aqueous (35%) solution of sodium hydroxide. The mixture was heated from room temperature to 85°C and kept for 3.5h. After that, the system was cooled down to room temperature by adding ice water. The resin was then dehydrated with rotary evaporation at 80°C until a viscosity of about 3500 mPas at 20°C was achieved. The solid content of the PUF resin prepared was 72%. The resin was kept at room temperature for 3 days before used for foaming.

Synthesis of organic PUF foam: 10 parts by weight of resin were mixed with 0.5 parts tween 80 as surfactant, 0.4-1.2 part (4-12 wt. %) of n-Pentane as blowing agent and 0.8-1.8 part (8-18 wt. %) of 65 % p-toluene sulfonic acid (pTSA) as curing agent in a beaker. n-Pentane was used as blowing agent because it has the low boiling point (36.1℃) that it can evaporate during the foaming process to producing a cellular structure. p-toluene sulfonic acid (pTSA) plays the role as catalyst to help the curing of PUF resin at low temperature. Then, fast stirring was maintained for around 2min at 25°C and then the mixture was immediately poured into a paper mould and placed in an oven for foaming and curing. Organic PUF foams with various densities were obtained by changing the concentration of the resin in the mixtures.

Synthesis of activated carbons foams from exemplar PUF foam: Monolithic activated carbons were prepared as follows: Firstly the exemplar organic PUF foam (see Figure 1) was carbonized in a horizontal tubular furnace at 900℃ under pure nitrogen environment and gradual increase of temperature (3℃/min). The carbon foams were then activated with CO_2 in a quartz tube heated from room temperature to 800℃. The CO_2 flow rate and N_2 flow rate were both 50ml/min. Depending on the duration of the activation, the activated carbon foams with various characteristics can be obtained. Fig. 1 shows an example of the organic foams prepared in this study before and after the mechanical measurement and also the activated carbon foams.

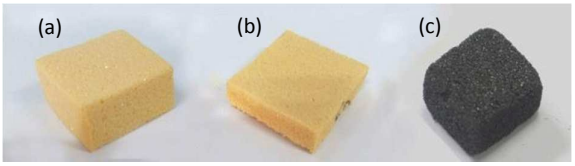

Figure 1. The photo of the exemplar organic foams before and after compression and also one of the activated carbon foam: (a) organic foam before compression measurement; (b) organic foam after compression measurement; (c) activated carbon foam.

Characterization of the developed foams

SEM and element analysis: The main intrinsic characteristics of the foams: cell structure, cell size were evaluated by SEM observation (FEG SEM Hitachi S 3400). Both secondary and backscattered electrons were used to get the images. Pore walls are very well defined using secondary electrons (SE), but struts and cell windows are much more clearly discernible with backscattered electrons (BSE). Nitrogen content was determined by Vario EL from Elementar.

Compression properties: Stress-strain of the developed materials under compression load was recorded with the CMT5000 Electronic Universal Testing Machine from Zhuhai SUST Electrical Equipment Ltd. The samples were cut for the dimensions of 30x30x15mm and the load rate was set at 2.0 mm/min. Each measurement was repeated 3-6 times. The ultimate load was taken at the point when the first layer of foam cells broke.

N_2 adsorption-desorption analysis: N_2 adsorption-desorption isotherms were obtained at 77K using a Micromeritics ASAP 2020 automatic apparatus. The samples were degassed for 24h under vacuum at 563K prior to any adsorption experiment. N_2 adsorption data were processed to generate : (i) surface area, S_{BET}, by the BET calculation method [22]; (ii) micropore volume, V_{DR}, according to the Dubinin-Radushkevich (DR) method [23]; (iii) total pore volume, $V_{0.99}$, defined as the volume of liquid nitrogen corresponding to the amount adsorbed at a relative pressure $P/P_0 = 0.99$ [24]. The average micropore diameter, L_0, [25] and the pore size

distributions (PSD) by application of the Density Functional Theory (DFT) [26] were also calculated.

Results and discussion

Apparent density of organic PUF foams: The apparent density of the foams is plotted as a function of the amount of blowing agent, the foaming temperature and also the mass of the curing agent (Fig. 2). The previous work of Zhao, et al. [27-28], based on mimosa tannin, demonstrated both theoretically and experimentally that the bulk density of tanning-based foams is inversely proportional to the amount of blowing agent. Plotting the inverse of the density as a function of the mass of blowing agent leads to a straight line with a correlation coefficient higher than 0.99 in this experiment. The same conclusion can be found with the impact of curing temperature from 60 to 80℃. However, for the influence of curing agent, the apparent density increased first and then decreased with the acid pTSA increased. It is considered that more curing agent at the beginning could accelerate curing process, leading to an increase in the density, but at the meantime, excess curing agent could also dilute the resin, resulting a decrease in the apparent density of final organic foams.

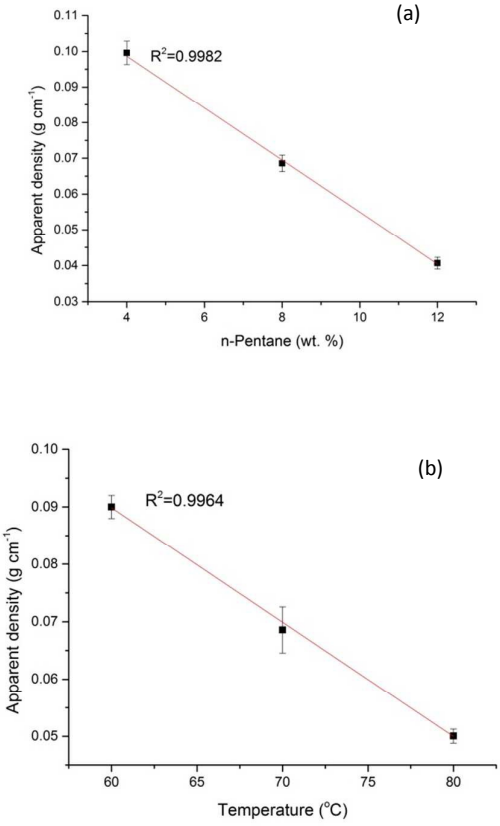

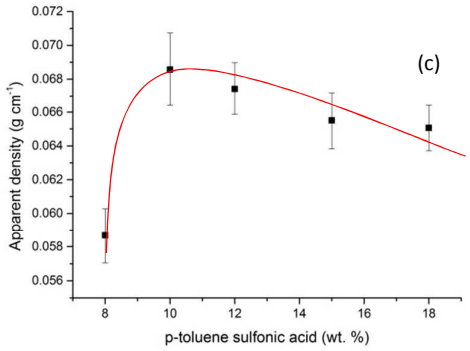

Figure 2. Apparent density of organic foams as a function of: (a) mass of blowing agent; (b) curing and foaming temperature; (c) mass of curing agent.

It must be noted that various formulations in this experiment allowed the control of apparent density of the developed organic foams, ranging from 0.04 to 0.12 g/cm^3. The exemplar organic foam (density =0.065g/cm^3) used for further preparing monolithic activated carbons foams in this study as an example has the formulation as follows: the mass of blowing agent is 0.8g, the curing and foaming temperature is 70℃ and the amount of curing agent is 1g.

Morphology and compressive strength of the developed organic PUF foams: The structure of the developed organic foam is presented in Fig. 3 at different magnifications. It is apparent that the foam has open porosities with more or less spherical bubble shapes, which are separated with each other by extremely thin, somewhat translucent, walls. Each cell is connected with its neighboring cells through more or less circular channels. The measured average pore diameter ranges from 100 to 600 um. The macropores connected with cell walls give more opportunity to react with activation agent in the activation process.

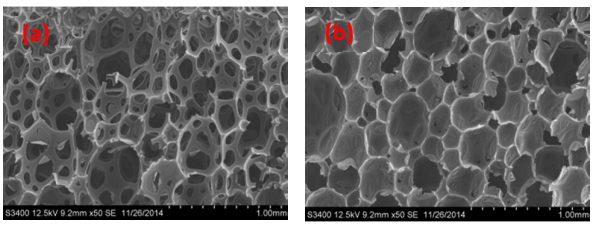

Figure 3. SEM images for exemplar organic foam (density = 0.065g/cm^3), the left image (a) was obtained with backscattered electrons at magnification 50×, that of the right (b) with secondary electrons at magnification 50×, respectively.

When subjected the organic foams to compression, the foam presented a brittle failure mode. The failure showed three distinct regions in the stress-strain curve (Fig. 4): linear elastic at low stresses, collapse and densification. The first zone, less than 20%, indicated the rupture of the weakest individual elements of the materials, producing struts and cell edges. A

samples	Activation time (min)	N content (%)	S_{BET} (m^2/g)	$V_{0.99}$ (cm^3/g)	V_{DR} (cm^3/g)	E_0 (kJ/mol)	Lo (nm)	$V_{DR}/V_{0.99}$ (cm^3/g)
Exemplar organic foam	0	4.50	<1	N	N	N	N	N
Carbon foam	0	1.75	<1	N	N	N	N	N
Activated carbons foams	4	1.58	771.11±3.91	0.36	0.31	26.49	0.72	0.86
	8	1.52	995.27±2.62	0.40	0.38	25.78	0.75	0.95
	10	1.49	1143.42±6.58	0.50	0.46	25.49	0.77	0.93
	20	1.48	1674.71±6.46	0.83	0.63	21.25	1.10	0.76

Table 1. N content and textural parameters of the activated carbons foams.

long serrated plateau at the second stage, typically ranging from 20% to 80% strain, originates from the coexistence of the collapsed and uncollapsed zones, typical feature of brittle foam undergoing successive cell wall fractures. Beyond the plateau, densification takes place and the stress rises sharply as soon as the densification begins, indicating that all the cell bands may have collapsed. These features are similar to those of phenol–formaldehyde foams and also tannin-based foams [30-32]. It is evident that there were the "noisy" aspect in the curve, this may be due to the redistribution of the compression after the facture of some layers of the cells: Once one cell layer collapsed, the compression load will redistribute on the subsequent cell layers. The maximum compression strength of the organic foam derived from the curve ranges from 0.17 to 0.67N/mm^2. Plotting the inverse of the compression strength as a function of the apparent density leads to a straight line with a correlation coefficient higher than 0.99 （not shown）. The exemplar organic foam presented the compression strength of 0.45N/mm^2. This fracture stresses are comfortably comparable to those of phenol foams [30-32].

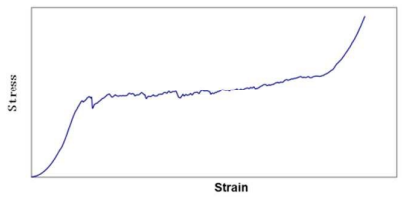

Figure 4. Stress–strain curve of compression for typical organic PUF foam.

The nitrogen content results from the element analysis show that the organic foam has nitrogen content 4.50%, so it can be used as a nitrogen containing precursor for preparing heteroatom containing activated carbons foams.

Characterization of monolithic activated carbon foams: The textural parameters determined by nitrogen adsorption at 77 K of four activated carbon foams were shown in Table 1. Those of exemplar organic foam and carbon foam are included for a comparison. The N content of exemplar organic foam was much higher than carbon and activated carbon foams, 4.50 %. The activated carbon foams had N content range from 1.48 to 1.58%. However, all the activated carbon foams had S_{BET} much higher, ranging from 770 to 1674 m^2/g, than those of organic and carbon foams, less than 1 m^2/g. They were mainly microporous with their micropore faction, $V_{DR}/V_{0.99}$, between 0.76 and 0.95. The impact of the activation time on the textural parameters was also significant, both the S_{BET} and V_{DR} increased with the increase of the activation time. The average pore width was in the range of 0.72 to 1.10 nm.

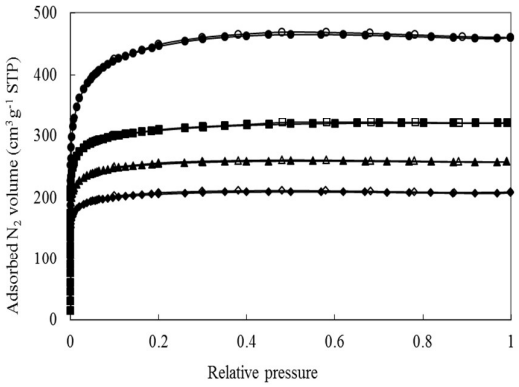

Figure 5. Nitrogen adsorption-desorption isotherms (empty and full symbols, respectively) at 77 K of activated carbon foams prepared with different activated time: (diamond) 4 min; (triangle) 8 min; (square) 10 min; (circle) 20 min.

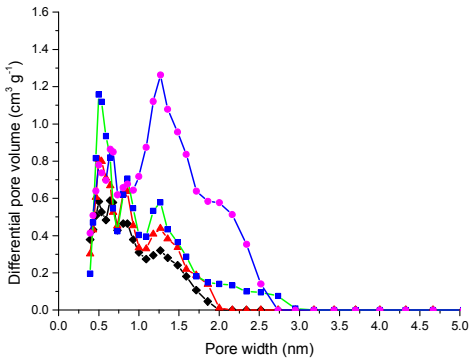

Figure 6. Pore size distributions of activated carbon foams prepared with different activated time. The symbols standing for activation time are the same as in Fig. 5.

The N_2 adsorption-desorption isotherms of the activated carbon foams at 77K were presented in Fig. 5. The isotherms are all type I according to the IUPAC classification. The main characteristics are the sharp increasing at a very low relative pressure and no hysteresis cycle. A scrutiny of the sorption behaviour at low pressure indicates that the N_2 adsorption may be much efficient in the micropores, much steeper increasing means more micropores inside the network structures of the developed activated carbon foams. The knee of the isotherms becomes wider with activation time, so the micropore width will become broadening. Fig. 6 shows the evolution of the pore size distribution (PSD) of the developed activated carbon foams. This reinforces and confirms the aforementioned findings that the activated carbon foams mainly have micropores and the micropore width becomes broaden with the activation time increased.

Comparison with open literature date: Table 2 present the typical nitrogen doped activated carbons from different precursors by different ways. We noticed that two dominant approaches to fabricate heteroatom-doped activated carbon have been developed: (i) carbonization/activation of heteroatom-enriched precursors [34-36, 38] and (ii) post-treatment of activated carbons with reactive heteroatom sources [37, 39-41, 49]. In most cases, nitrogen-doped activated carbons were achieved by introducing nitrogen through the post treatment methods like treated with ammonia gas or urea. It was proved that these post treatment not only modify their surface chemistry but also their porous texture. The pores produced by activation may block by the heteroatom sources [37]. Further, the use of toxic reactive gas (e.g., NH3 or HCN for N-doping) makes researchers hesitate to choose this approach [39, 41]. The other case is to use the solid reactant as nitrogen resource [37], like urea and melamine, but cannot apply to monolithic carbons. However, the drawbacks can be overcome by employing N-containing materials as precursors [26]. Compared with conventional nitrogen doped ACs, the use of N-containing PUF resin as precursors makes it easy to control the heteroatom containing. Meanwhile, the resin precursor copolymerized with one or more additional modifiers (urea in current work) is handy in process. Once the precursor of PUF foam is provided, only one-step activation under inert gas atmosphere is necessary for heteroatom-doped activated carbons foams, thus without the post-modification. So in this work, for the monolithic bimodal cellular activated carbon foams production, we chose the approaches of using nitrogen-containing PUF foams as precursor. From Table 2, we observed that the monolithic activated carbon foams are comfortably comparable to those of nitrogen doped activated carbons, but with bimodal cellular structure.

Table 2 comparison of activated carbons doped with nitrogen

Precursors	Post treatment	Nitrogen content (Wt. %)	Surface area (m^2/g)	Ref.
PUF foam	without	1.50	1674	This work
melamine-modified PF resins	without	1.00	1439	34
Polyaniline	without	3.20	1805	35
polyphosphazene	without	5.40	1341	36
aminophenol/formaldehyde resin	without	4.06	226	38
ACs from Coal	thermal treatment with urea	8.78	2737	37
ACs from RF gels	thermal treatment with $NaNH_2/NH_4Cl$	1.60	1938	39
ACs from Hay	urea solution	1.59	111	40
ACs	ammonia gas	4.40	N	41

Table 3 summarized all the monolithic cellular activated carbons prepared from different carbon foams in the open literature [8, 33, 42-47]. As mentioned, the carbon foams usually have low density, high porosity, but with very low surface area. So the thermal activation for the enhancement of specific surface area is necessary. From table 3, It is obvious that two approaches can use to fabricate activated carbon foams: physical (CO_2, steam and air) and chemical (KOH, $ZnCl_2$) methods. All the prepared activated carbon foams present the bimodal cellular structure, the interconnected macroporous and micro/meso- porosity structures, but most of them shown no nitrogen containing [8, 33, 42-47]. The activated carbon foam from pitch-based carbon foam had nitrogen content 1.2 wt. % due to the post-treatment with nitric acid [42]. Therefore, only our work prepared nitrogen doped activated carbon foam directly from carbon precursors containing

nitrogen. The BET surface area of our sample was also the highest within the physical activation. So for sure, the activated carbon foam from current work with the highest surface area, nitrogen containing and bimodal cellular structure give them the potential of higher adsorption kinetics and some special applications.

Table 3 the cellular activated carbon foam prepared from different carbon foams

Precursors	Activation methods	Nitrogen content (wt. %)	Surface area (m^2/g)	Ref.
PUF foam	CO_2	1.5	1674	This work
PF foam	steam	N	728	8
Pitch-based carbon foam	steam	1.2	933	42
liquefied birch sawdust-based foam	steam	N	555	43
liquefied larch sawdust-based foam	KOH	N	1918	44
SiC foam	steam	N	680	45
Tannin foam	$ZnCl_2$	N	1875	46
Tannin foam	steam	N	1078	33
Polyimide impregnated foams	air	N	1540	47

Conclusions

The organic foam has been firstly synthesized from phenol–urea–formaldehyde resin under alkali condition. The apparent density of organic foams could be controlled in the range of 0.04-0.12g/cm^3 by changing the formulation, corresponding to the compression strength from 0.17 to 0.67N/mm^2. The developed foams had a fully connected network of cells with diameter of 100-600um. A novel monolithic nitrogen-containing microporous activated carbon was then successfully prepared by the carbonization and CO_2 activation processes from organic foam. The developed carbons have achieved apparent surface area as high as 1674 m^2/g and microporous volume as high as 0.86cm^3/g, similar to that of many commercial carbonaceous adsorbents, but with nitrogen content around 1.5 wt. %. These materials were expected to have higher adsorption kinetics and some special applications due to the heteroatom nitrogen introduced and monolithic shape with bimodal cellular structure.

Unlike the usual adsorbents, the micro/meso- porosity is fully accessible in these new activated carbon foams, indicating potentially high adsorption or catalysis kinetics due to little diffusion limitation. The materials could be used as power form or monolithic shape, depending on the different applications. Experiments on the determination of adsorption kinetics and enhancing of performance by nitrogen doping are currently in progress.

Acknowledgements

The present research was supported by the National Natural Science Foundation of China (31300488), and Fujian Agriculture and Forestry University Fund for Distinguished Young Scholars (xjq201420).

Notes and references

1 V. K. Gupta, A. Nayak, S. Agarwal and I. Tyagi. Journal of colloid and interface science, 2014, 417, 420-430.
2 Y. Xiang, L. Kong, P. Xie, T. Xu, J. Wang and X. Li. Industrial & engineering chemistry research, 2014, 53(6), 2197-2203.
3 W. Zhao, V. Fierro, C. Zlotea, E. Aylon, M. T. Izquierdo, M. Latroche and A. Celzard. International journal of hydrogen energy, 2011, 36(9), 5431-5434.
4 V. J. Watson, C. Nieto Delgado and B. E. Logan. Environmental science & technology, 2013, 47(12), 6704-6710.
5 S. Sircar, T. C. Golden and M. B. Rao. Carbon, 1996, 34(1), 1-12.
6 A. Oya, S. Yoshida, J. Alcaniz-Monge and A. Linares-Solano. Carbon, 1995, 33(8), 1085-1090.
7 N. P. Wickramaratne and M. Jaroniec. Journal of Materials Chemistry A, 2013, 1(1), 112-116.
8 X. Zhao, S. Lai, H. Liu and L. Gao. Journal of Environmental Sciences, 2009, 21, S121-S123.
9 H. Teng and S. C. Wang. Carbon, 2000, 38(6), 817-824.
10 G. Du, H. Lei, A. Pizzi and H. Pasch. Journal of Applied Polymer Science, 2008, 110(2), 1182-1194.
11 A. Pizzi A, A. Stephanou, I. Antunes and G. De Beer. Journal of Applied Polymer Science, 1993, 50, 2201-2207.
12 C. Zhao, A. Pizzi and S. Garnier. Journal of Applied Polymer Science, 1999, 74, 359–378.
13 C. Zhao, A. Pizzi, A. Kuhn and S. Garnier. Journal of Applied Polymer Science, 2000, 77, 249–259.
14 W. Xing, C. Liu, Z. Zhou, L. Zhang, J. Zhou, S. Zhuo, Z. Yan, H. Gao, G. Wang and S. Qiao. Energy & Environmental Science, 2012, 5(6), 7323-7327.
15 J. Jiang, Q. Gao, Z. Zheng, K. Xia and J. Hu. International journal of hydrogen energy. 2010, 35, 210-216.
16 Z. Zhou, X. Gao, J. Yan and D. Song. Carbon 2006, 44, 939-947.
17 K. S. W. Sing, D. H. Everett and R. A. W. Haul. Pure and applied chemistry, 1985, 57: 603.
18 B. Del Saz-Orozco, M. V. Alonso, M. Oliet, J. Carlos Domínguez and F. Rodriguez. Composites Part B: Engineering, 2014, 56, 546-552.
19 B. Del Saz-Orozco, M. Oliet, M. V. Alonso, E. Rojo and F. Rodríguez. Composites Science and Technology, 2012, 72(6), 667-674.
20 B. Grindatto, A. Jourdan and M. Prin. Process for the preparation of metal carbides having a large specific surface from activated carbon foams: U.S. Patent 6,217,841.
21 C. Yang, Y. Sun, X. Bing and Y. LV. Journal of functional materials, 2010, 41, 165-168.
22 S. Brunauer, P.H. Emmet and E. Teller. Journal of the american chemical society, 1938, 60, 309–319.
23 M. M. Dubinin. Carbon, 1989, 27, 457–467
24 S.J. Gregg and K.S.W. Sing. Adsorption, surface area and porosity. (2nd ed.) Academic Press, London (1982).
25 F. Stoeckli, A. Slasli, D. Hugi-Cleary and A. Guillot. Microporous and mesoporous materials, 2002, 51, 197–202.
26 P. Tarazona. Surface Science, 1995, 331–333, 989–994.
27 W. Zhao, A. Pizzi, V. Fierro, G. Du and A. Celzard. Materials Chemistry and Physics, 2010, 122, 175-182.

28 W. Zhao, V. Fierro, A. Pizzi, G. Du and A. Celzard. Materials Chemistry and Physics, 2010, 123, 210-217.
29 H. Shen and S. Nutt. Composite. A, 2003, 34, 899–906.
30 M.H. Okzul and J.E. Mark. Polymer engineering and science. 1994, 34, 794–798.
31 V.K. Rangari, T.A. Hassan, Y. Zhou, H. Mahfuz, S. Jeelani and B.C. Prorok. Journal of applied polymer science. 2007, 103, 308–314.
32 C. Gontier, A. Bouchou and C. Vinot. International journal of mechanical sciences, 2001, 43, 2371–2384.
33 W. Zhao, V. Fierro, A. Pizzi and A. Celzard. Journal of Materials Science, 2010, 45, 5778–5785.
34 RL. Tseng, FC. Wu and RS. Juang. Separation & Purification Technology, 2015, 140, 53–60.
35 A. Silvestre-Albero, J. Silvestre-Albero, M. Martinez-Escandell, M. Molina-Sabio, A. Kovacs and F. Rodriguez-Reinoso. Microporous and Mesoporous Materials, 2015, 218, 199–205.
36 J. Jiang, H. Chen, Z. Wang, L. Bao, Y. Qiang, S. Guan and J. Chen. Journal of Colloid and Interface Science, 2015, 452, 54–61.
37 W. Zhao, V. Fierro, N. Fernández-Huerta, M.T. Izquierdo and A. Celzard. International Journal of Hydrogen Energy, 2013, 38, 10453-10460.
38 Y. Li, S. Zhang, H. Song, X. Chen, J. Zhou and S. Hong. Electrochimica Acta, 2015, 180, 879–886.
39 H George，D Takeru，K Kazuyoshi，K Yoji，K Hiroshi, A. Takeshi, and N. Kazuki. Chemistry of Materials, 2015, 27, 4703–4712.
40 J. Kazmierczak-Razna, P. Nowicki and R. Pietrzak. Powder Technology, 2015, 273, 71-75.
41 R.J.J. Jansen and H. van Bekkum. Carbon, 1994, 32, 1507-1516.
42 B. Tsyntsarski, B. Petrova, T. Budinova, N. Petrov, LF. Velasco, JB. Parra, and CO. Ania. Microporous and Mesoporous Materials, 2012, 154, 56-61.
43 R. Wang, W. Li and S. Liu. Journal of Materials Science, 2012, 47, 1977-1984.
44 S. Liu, Z. Huang and R. Wang. Materials Research Bulletin, 2013, 48, 2437-2441.
45 B. Grindatto, A. Jourdan and M. Prin. Process for the preparation of metal carbides having a large specific surface from activated carbon foams: US, US6217841. 2001.
46 G. Tondi, A. Pizzi, L. Delmotte, J. Parmentier and R. Gadiou. Industrial Crops and Products, 2010, 31, 327-334.
47 N. Ohta, Y. Nishi, T. Morishita, Y. Ieko, A. Ito A and M. Inagaki. New Carbon Materials, 2008, 23, 216–220.
48 S.R. Tennison. Applied Catalysis A: General, 1998, 173, 289-311.
49 H. George, D. Takeru, K. Kazuyoshi, K. Yoji, K. Hiroshi, A. Takeshi and N. Kazuki. Chemistry of Materials, 2015, 27, 4703-4712.